GA–C23890

A NEW LAYERING METHOD FOR INDIRECT DRIVE IFE TARGETS

PROGRESS REPORT FOR THE PERIODS AUGUST 15, 2000 through DECEMBER 14, 2001

by

PROJECT STAFF

Prepared for the
Office of Fusion Energy Sciences
Grant No. DE-FG03-00ER54595
for U.S. Department of Energy

DECEMBER 2001

GENERAL ATOMICS

GA–C23890

A NEW LAYERING METHOD FOR INDIRECT DRIVE IFE TARGETS

PROGRESS REPORT FOR THE PERIODS AUGUST 15, 2000 through DECEMBER 14, 2001

by

PROJECT STAFF

Prepared for the
Office of Fusion Energy Sciences
Grant No. DE-FG03-00ER54595
for U.S. Department of Energy

GENERAL ATOMICS PROJECT 30077
DECEMBER 2001

A NEW LAYERING METHODS FOR INDIRECT DRIVE IFE TARGETS

Year 1 Progress Report
April 15, 2001
Principal Investigator: D.T. Goodin
Other Participants: M. Tillack, J. Pulsifer, R.W. Petzoldt, C. Gibson, G. Besenbruch
General Atomics

ABSTRACT

Layering is the process whereby condensed deuterium tritium (DT) fusion fuel at 18-19 K is very uniformly distributed on the inside wall of an Inertial Fusion Energy (IFE) target. The quality and uniformity of the DT layer has a profound effect on the performance (gain) of the target. It would be a great advantage for indirect drive targets to carry out layering with the capsule already assembled in the hohlraum. One concept to accomplish this is to layer targets in controlled temperature, cryogenic tubes while they are being staged for feeding to the injection system.

In this report we have demonstrated through extensive analysis that in-hohlraum layering is possible, but that variations in dimensions, alignments and material properties can easily cause the capsule temperature nonuniformity to exceed values needed to assure proper fuel layering. The concept shows sufficient promise to warrant continued investigation. Analysis alone cannot demonstrate the feasibility of in-hohlraum layering. One of the most basic and important experiments is the measurement of the properties of hohlraum materials. Such measurements must be performed with sufficient accuracy to demonstrate predictability and repeatability to the level of precision needed to maintain thermal control. Continued close interaction between target designers and target fabricators is needed to ensure development of a cost-effective target design

1. Introduction

Fuel layering is an essential step for any of the target designs under consideration for Inertial Fusion Energy (IFE), for both direct and indirect drive targets. The uniformity of the DT layer can have a profound effect on the gain of the target. Currently demonstrated layering methods require placement of bare capsules in a "layering sphere" to control DT surface temperature uniformity to less than ~100 μK for times up to several hours. Staging individual capsules in layering spheres would require a prohibitively large number of spheres to produce targets at IFE rates (~500,000 per day). An additional step to rapidly assemble the capsule and hohlraum after layering also would be required.

Layering indirect drive targets with the capsule already assembled in the hohlraum would be a distinct advantage. One way to accomplish this is to layer fully-assembled targets in controlled temperature tubes while they are being staged for feeding to the injection system. Successful layering requires maintaining a specially tailored temperature profile on the hohlraum surface. Tritium decay heat removal from the filled capsule depends upon the thermal properties of the tube material, the capsule material, and the other materials filling the hohlraum.

In this work we evaluate various techniques for achieving adequate thermal control during the in-hohlraum layering process. The reference technique is application of a predetermined temperature profile along the hohlraum outer surface using a passive control system. Anisotropic material properties also have been studied as a possible supplemental technique for tailoring the profiles. This is especially important for high-conductivity materials such as gold, which interfere with external control techniques. Recommendations are made to target designers on techniques which will be important in order to make in-hohlraum layering possible.

2. Thermal Analysis

2.1. Background

2.1.1. Geometry

The reference geometry for all thermal analysis shown here is the "distributed radiator" design of Callahan-Miller (see Figure 1) [1]. The target consists of a DT capsule surrounded by either a Be or plastic ablator, various low-density foams designed to absorb and re-radiate the ion beam energy, and a Flibe outer covering for mechanical stability and compatibility with the assumed chamber protectant. Table 1 summarizes the material composition and density of each zone.

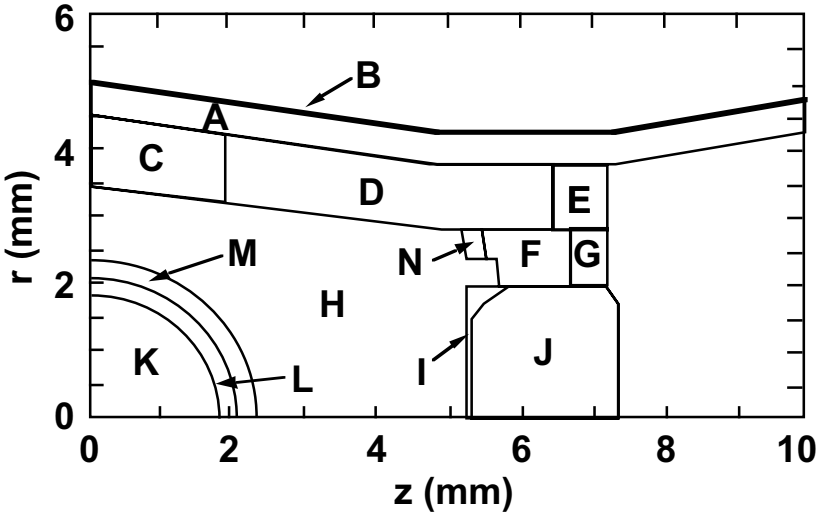

Figure 1. Distributed radiator indirect drive target [1].

Table 1. Reference composition of the distributed radiator target

Zone	Composition	Density
A	AuGd	0.1 g/cm^3
B	AuGd	13.5 g/cm^3
C	Fe	16 mg/cm^3
D	$(CD_2)_{0.97}Au_{0.03}$	11 mg/cm^3
E	AuGd	0.11 g/cm^3
F	Al	70 mg/cm^3
G	AuGd	0.26 g/cm^3
H	CD_2	1 mg/cm^3
I	Al	55 mg/cm^3
J	AuGd sandwich	0.1, 1.0, 0.5 g/cm^3
K	DT	0.3 mg/cm^3
L	DT	0.25 g/cm^3
M	$Be_{0.995}Br_{0.005}$	1.845 g/cm^3
N	$(CD_2)_{0.97}Au_{0.03}$	32 mg/cm^3

2.1.2. Uniformity Goal

The primary objective of this study is to establish and demonstrate techniques which will allow adequate control over the temperature of the DT fuel such that the uniformity of the fuel under beta layering will meet symmetry requirements imposed by the physics of target implosion [2]. Recent analysis suggests that IFE targets are much less susceptible to DT ice roughness as compared with ignition targets (*e.g.*, NIF), especially for the low mode-number perturbations which arise due to temperature variations at the hohlraum surface [3]. Roughness values as high as 5-10 μm may be acceptable.

A simple estimate of the thermal asymmetry associated with this level of thickness variation is obtained by assuming the temperature at the inner surface is held constant due to mass transfer by sublimation and condensation, and the temperature rise through the fuel layer is due to internal heating (q'''):

$$\Delta T = q''' L^2 / 2k$$

where L is the fuel thickness and k is the fuel thermal conductivity. For small perturbations in thickness (δ), the perturbation in ΔT (ξ) can be expressed as:

$$\xi = q''' L \delta / k$$

Figure 2 indicates that a temperature variation around the outer surface of the DT ice of ~250 μK can be tolerated if a 5 μm thickness variation is acceptable.

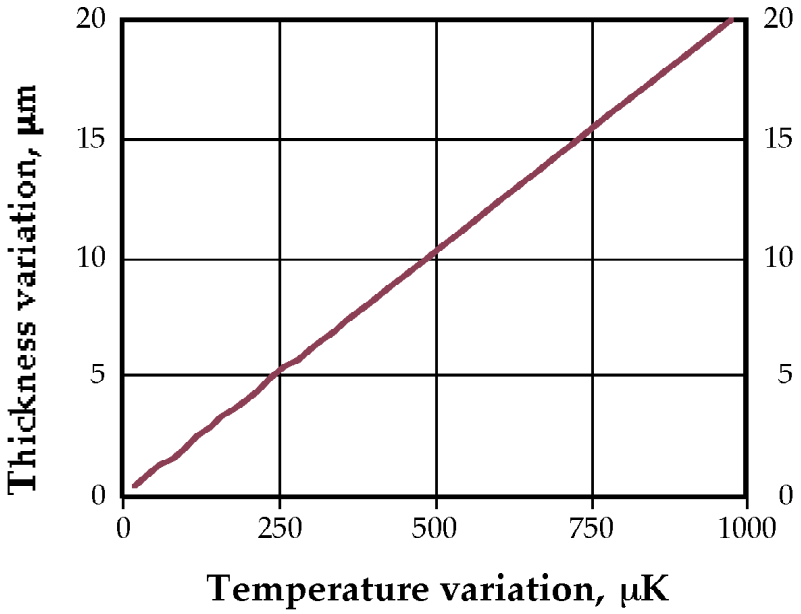

Figure 2. Change in DT ice thickness corresponding to a small change in through-thickness temperature drop.

2.1.3. Overview of Analyses Performed

Several variations were analyzed in an attempt to determine the most effective technique for providing uniform layering:

1. First, a uniform hohlraum boundary temperature was applied with Be and plastic capsules surrounding the DT fuel. The Be capsule has sufficient conductivity such that acceptable temperatures are achieved even in this case of uniform boundary temperature. Detailed comparisons were made with the work of Siegel [4] to establish the validity of the analysis technique. The case of a plastic ablator exhibited far greater nonuniformity in the fuel temperature, such that some form of thermal control becomes necessary.

2. In order to estimate the hohlraum surface temperature variation needed to assure relatively uniform DT surface temperature, an "inverse analysis" was performed. In this case, the DT surface temperature was forced to be uniform and the resulting temperature profile at the hohlraum surface was obtained with minimum resistance to heat flow outside the hohlraum. While an exact solution is not possible using this technique, the result was used as an initial estimate and subsequent iterations established a closer fit to the optimum solution.

3. The primary alternative to external temperature control which was explored is internal manipulation of the geometry and thermophysical properties of the hohlraum materials. One of the most obvious areas needing improvement is the solid-density Au outer layer (zone B) which tends to create an isothermal surface, thus preventing effective external control. Breaking the Au into segments or otherwise creating anisotropic conductivity was shown to be very effective. Manipulation of the low-density foams was explored as an additional technique. Anisotropic conductivity was applied to zones A, E, F, G, I, and J. This technique proved less effective than external temperature control.

4. Integrated analysis was performed on the hohlraum including the surrounding cryogenic pipe and thermal contact material in order to demonstrate the feasibility of the proposed final design solution.

5. Finally, analyses were performed in order to determine the sensitivity of the result to uncertainties in the properties and geometry. The main concerns examined here were:
   - variations in thermal conductivity of selected zones (§2.7.1),
   - variations in temperature profile applied to the outer hohlraum surface (§2.7.2),
   - variations in alignment of the hohlraum with the staging tube (§2.7.3).

2.2. Analysis of Targets with Uniform Boundary Temperature

In order to bound the severity of the problem and establish a baseline for comparison, analysis was performed on targets with uniform temperature applied to the outer surface of the hohlraum. Both Be and plastic ablators were examined.

The axisymmetric thermal model used in ANSYS® calculations is shown in Figure 3. Automatic mesh generation was used. Temperature dependent properties were collected in Ref. [4] and Appendix A.

The gold layer (zone B) is too thin to discretize accurately, so it was modeled with a thicker region having parallel and perpendicular thermal conductivities tailored to match the thermal response of the true material.

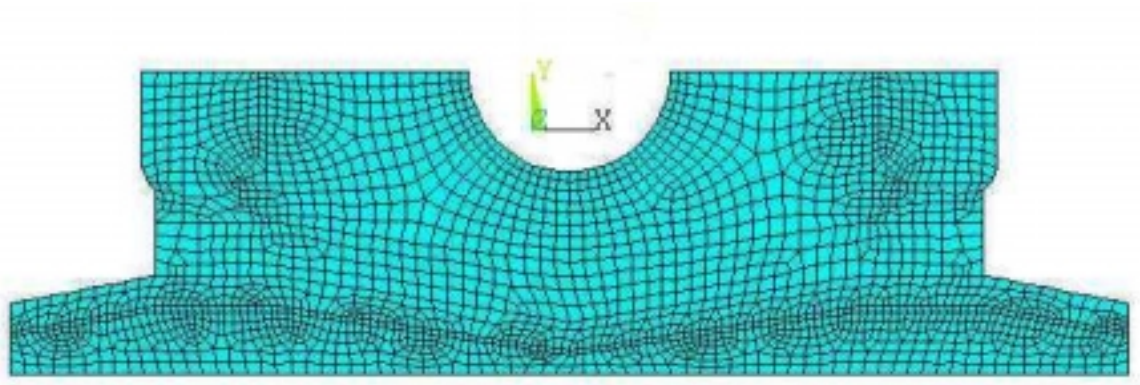

Figure 3. ANSYS® thermal model of the distributed radiator indirect drive target.

2.2.1. Results with a Be ablator

The beryllium ablator target was modeled using the mesh in Figure 3, but with material properties set according to the zones in Figure 1 as follows: the region outside of layer B is Flibe, region B is gold, region L is DT, region M is Be, and all other regions are modeled with properties of pure helium gas. This is the same assumption used by Siegel [4]; the materials used in constructing the hohlraum have such low density and poor interconnectivity that the solid phase is assumed to make no contribution to heat transfer. Our model has been slightly modified as compared with Siegel to include helium fill outside the ends of the hohlraum in order to facilitate a symmetry condition for the case where multiple hohlraums are stacked end-to-end in a layering tube.

Heat generation of 48,700 W/m^3 was applied to zone L, modeling heat produced by tritium decay, and a constant temperature of 19.2 K was prescribed at the hohlraum outer surface. Adiabatic boundaries were prescribed at the ends of the hohlraum.

The resulting heat fluxes and temperatures in the hohlraum are shown in Figures 4 and 5, respectively. Figure 6 shows the nodal temperature distribution near the capsule, while Figure 7 is a plot of the nodal temperatures along the outer DT surface from θ=0 to π. Variation in temperature is of the order of 2 μK. Figure 5 closely matches Figure 7.3 of Siegel [4]; the temperature difference does not exceed 3 μK. The close match allows us to use the Be ablator model as a baseline for the remainder of our analysis.

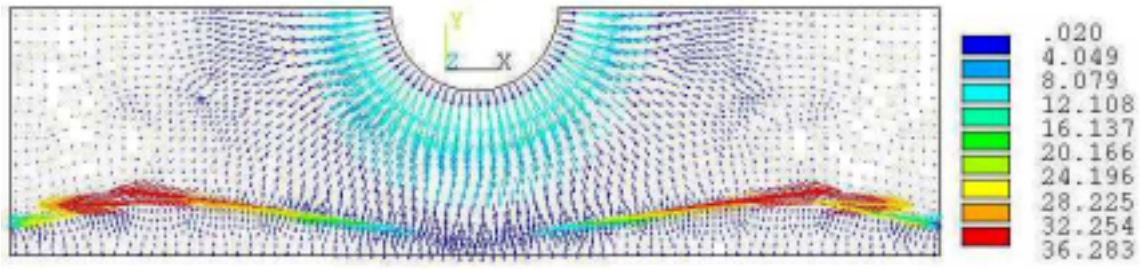

Figure 4. Heat fluxes in the hohlraum with a Be ablator (K).

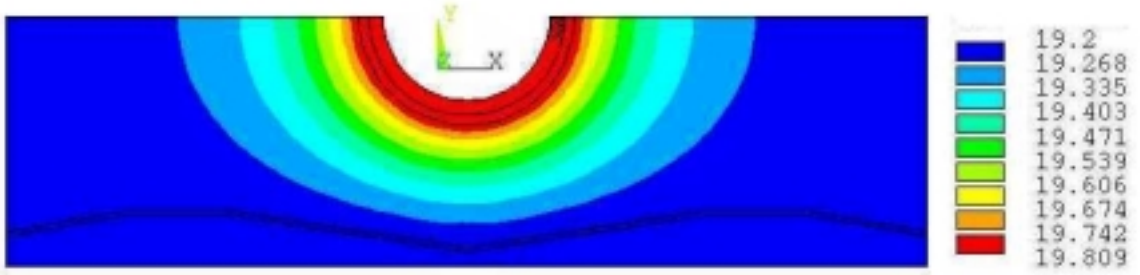

Figure 5. Temperatures in the hohlraum with a Be ablator (K).

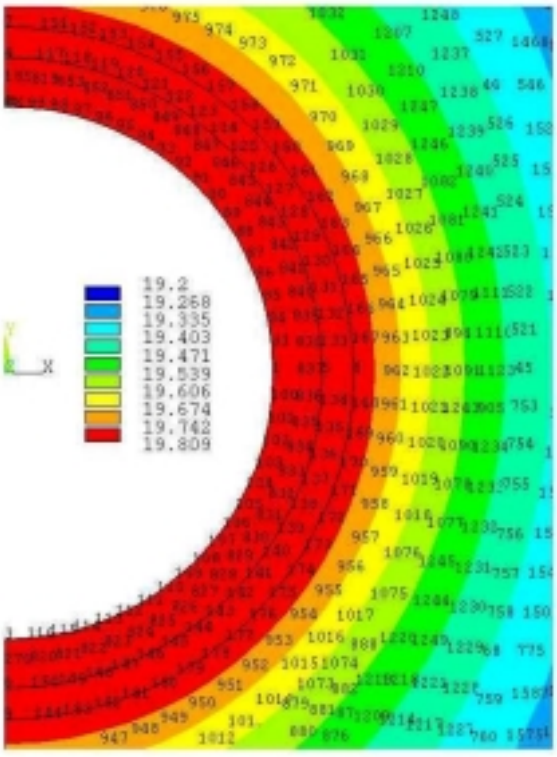

Figure 6. Temperatures near the capsule with a Be ablator (K).

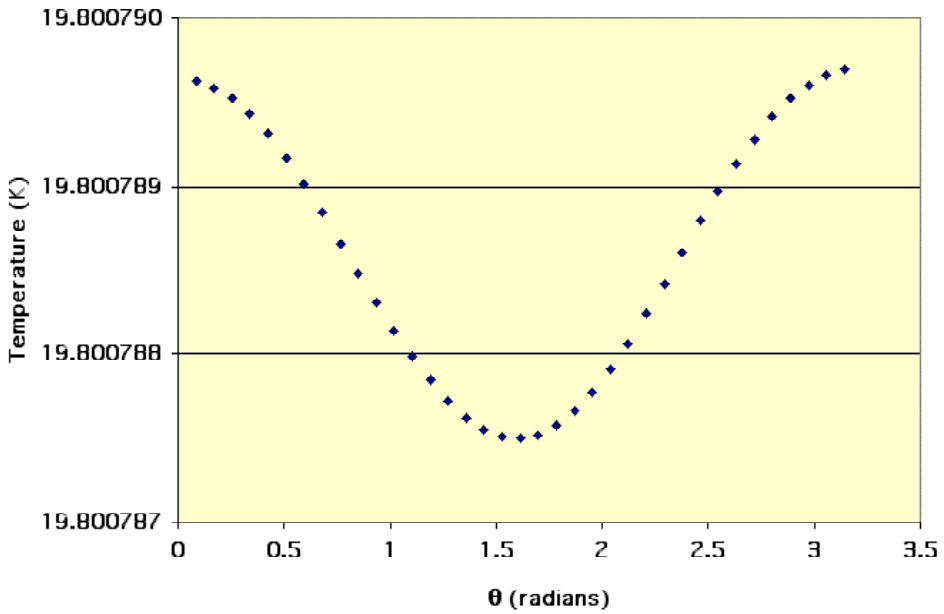

Figure 7. Temperatures at the DT-to-Be interface.

2.2.2. Results with a plastic ablator

The plastic ablator target was also modeled using the mesh in Figure 3, with the same material properties as the Be benchmark except replacing the properties of Be with those of polystyrene. The same heat generation and temperature boundary condition used in the Be benchmark were applied.

Heat fluxes and temperatures in the hohlraum are shown in Figures 8 and 9, respectively. Figure 10 shows the nodal temperature distribution near the capsule while Figure 11 is a plot of the nodal temperatures along the outer DT surface from $\theta=0$ to π. Variation in temperature is of the order of 10 mK. This also matches the work of Siegel [4], where a temperature difference of 0.01 K was found along the DT surface.

The thickness variation resulting from this temperature variation – shown in Figure 12 – is of the order of 200 μm, which is a large fraction of the total fuel thickness. Clearly, some additional comtrol over the DT temperature profile would be needed in this case.

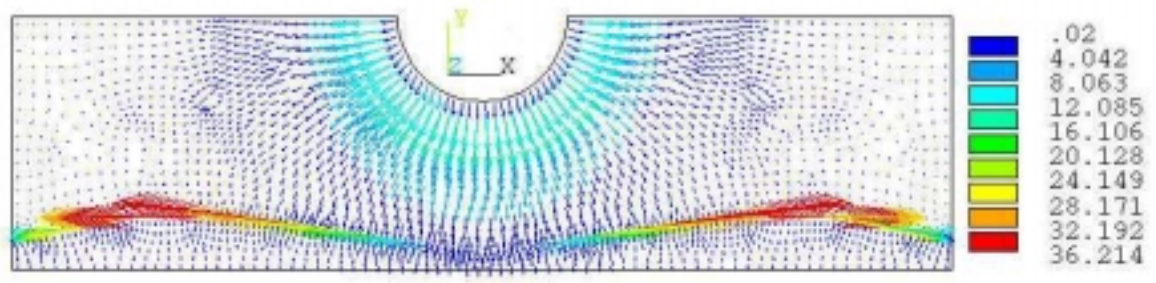

Figure 8. Heat fluxes in the hohlraum with a plastic ablator.

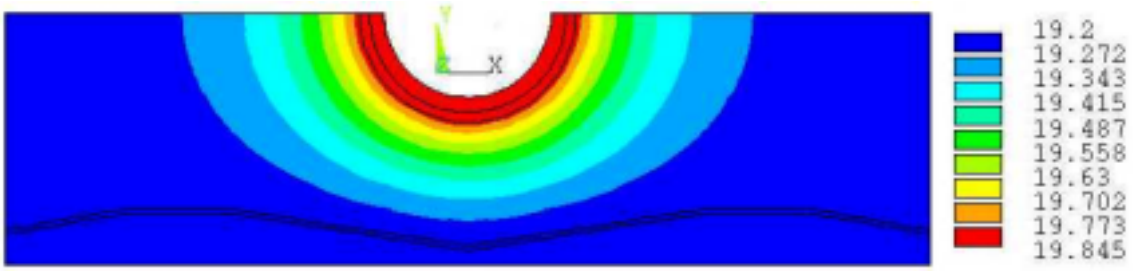

Figure 9. Temperatures in the hohlraum with a plastic ablator (K).

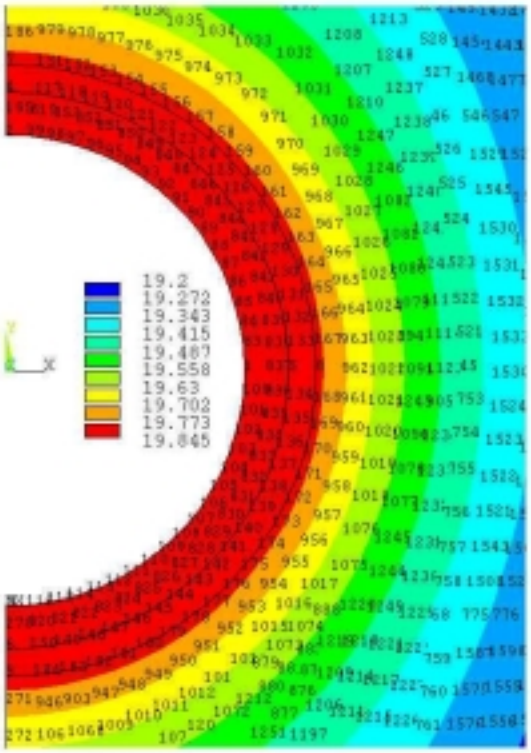

Figure 10. Temperatures near the capsule with a plastic ablator (K).

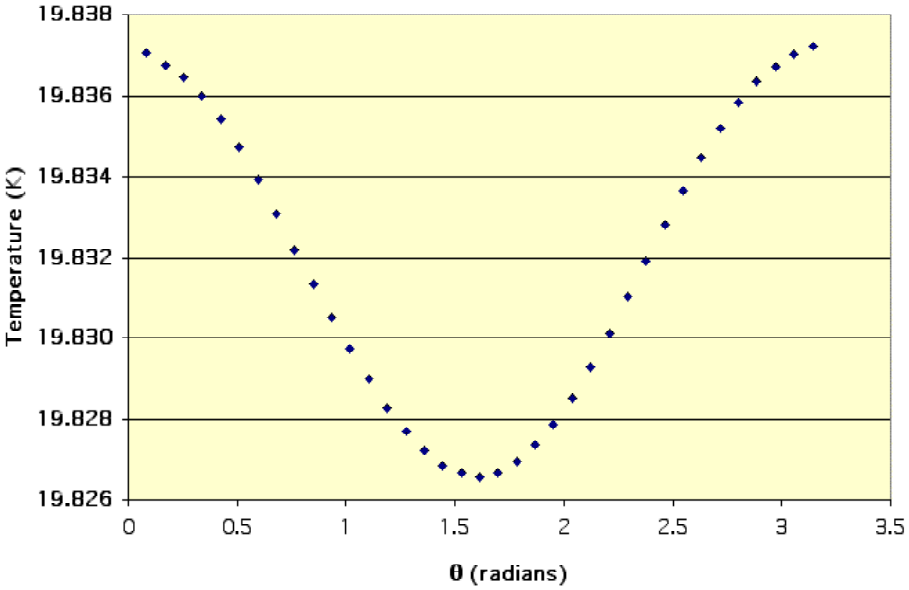

Figure 11: Temperatures at the DT-to-plastic interface.

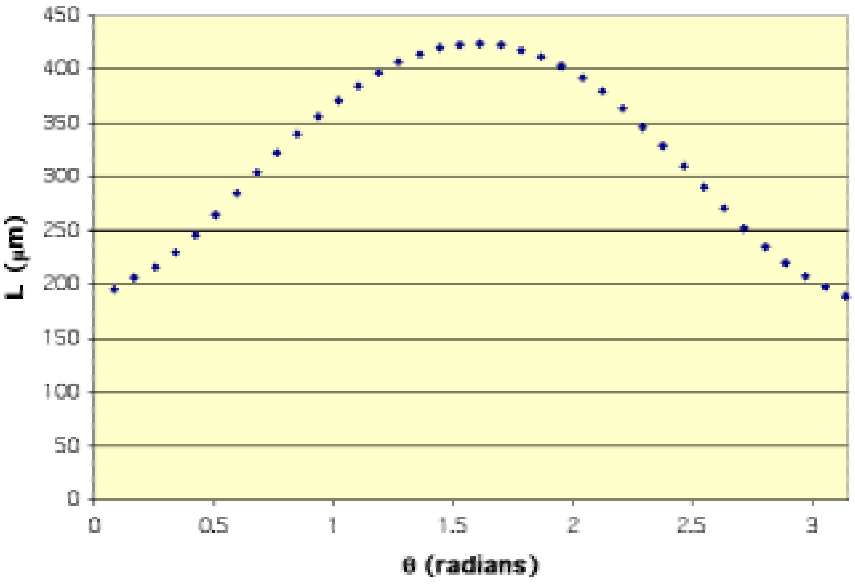

Figure 12: Variation of the DT thickness for the plastic ablator target with uniform applied hohlraum temperature.

2.3. Modification of the gold layer to allow thermal penetration

Initial attempts were made to reduce the temperature variation along the DT surface by imposing a spatially varying temperature along the outer surface of the hohlraum. Varying the hohlraum outer surface temperature as much as several degrees along the length of the hohlraum had little effect at the DT because the layer of AuGd in region B was masking any attempt to control the temperatures inside of it. Figures 4 and 8 clearly show that large heat flows appear within this zone. The AuGd layer attempts to maintain an isotherm, in competition with the external control system.

This problem was corrected by assuming that region B could be designed such that heat flux would flow easily across the layer and not along it (possibly by chopping it at small intervals or by manufacturing it with anisotropic properties). With anisotropic properties in region B, applied temperature profiles along the outer hohlraum surface were found to make profound differences in the temperature distribution at the DT.

Figure 13 shows the hohlraum temperature distribution before and after segmentation of the AuGd layer. The results clearly show how segmentation allows penetration of the external temperature profile into the bulk of the hohlraum.

2.4. Inverse Thermal Problem

The correct temperature profile to apply along the hohlraum surface could be determined by trial and error. However, a more efficient technique was used in order to obtain a relatively accurate first estimate. A thick zone of material was added to the outer surface of the hohlraum in order to minimize the effect of the boundary. A fixed uniform temperature (equal to the desired temperature under ideal conditions) was applied to the DT outer surface, and a uniform heat flux boundary condition was applied to the outer boundary of the solution domain with a value consistent with the total volumetric heat generation in the DT. In this way, a temperature profile compatible with a uniform DT temperature naturally results on the hohlraum surface. This profile is not the exact solution for the thermal control system because the heat fluxes at the hohlraum surface are not the same; however, it provides a good first estimate which can be optimized by iteration. In fact, as seen below, this first estimate is sufficiently accurate to meet the requirements for DT thickness uniformity. Figure 14 shows the full result of the inverse thermal problem and Figure 15 shows the temperature distribution along the hohlraum surface in more detail.

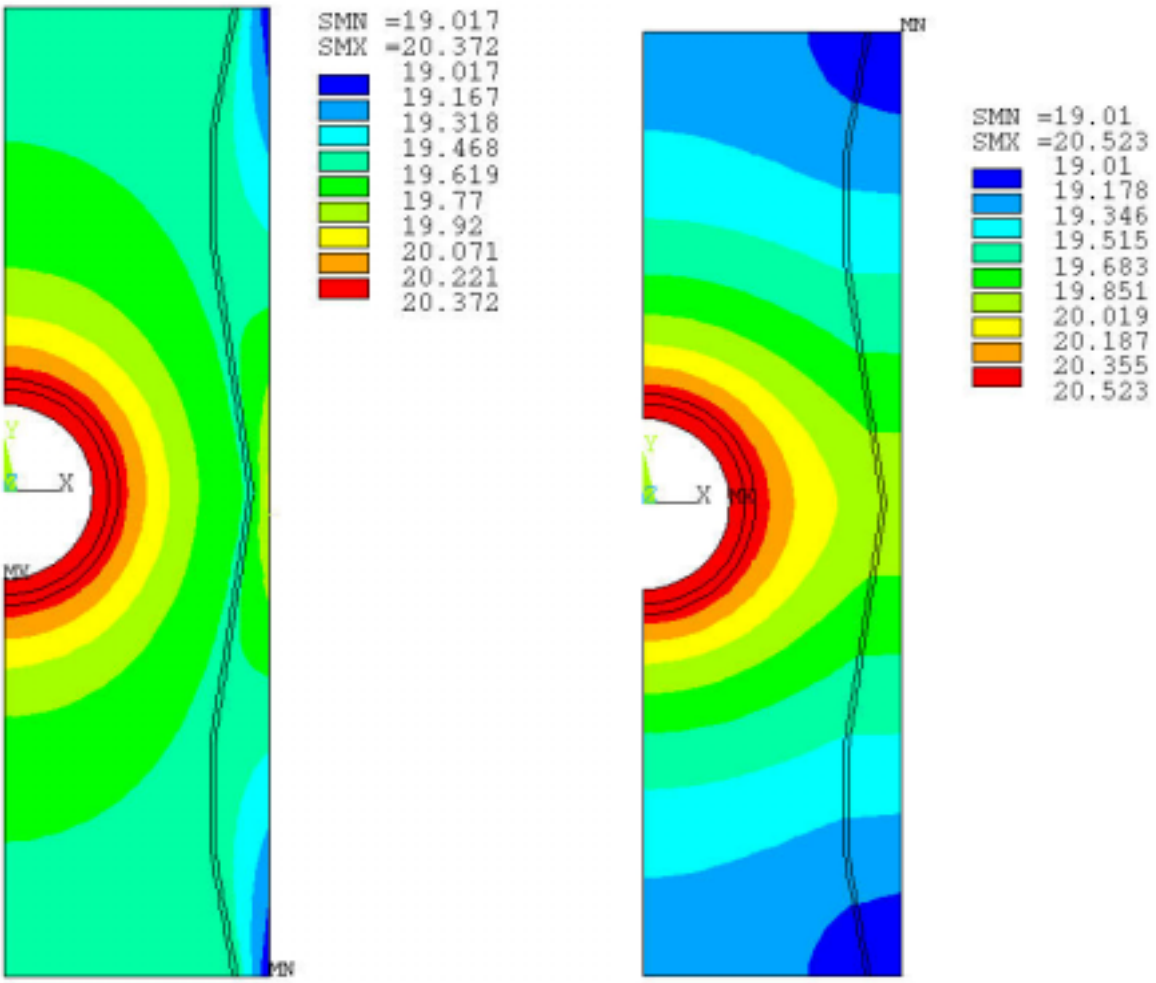

Temperatures with continuous AuGd (K). Temperatures with segmented AuGd (K).

Figure 13. Effect of cutting the AuGd layer.

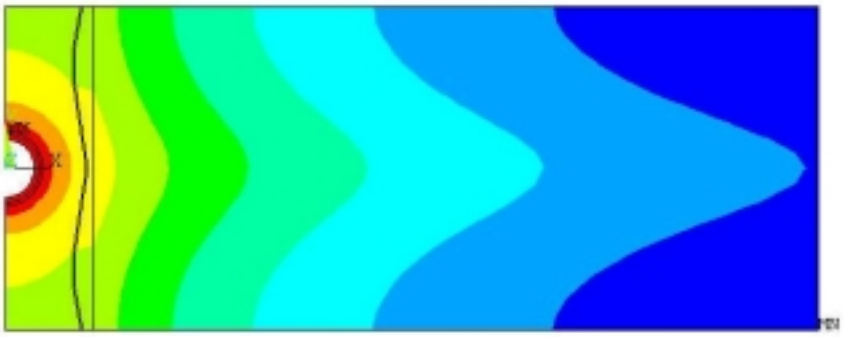

Figure 14. Solution of the "inverse thermal problem."

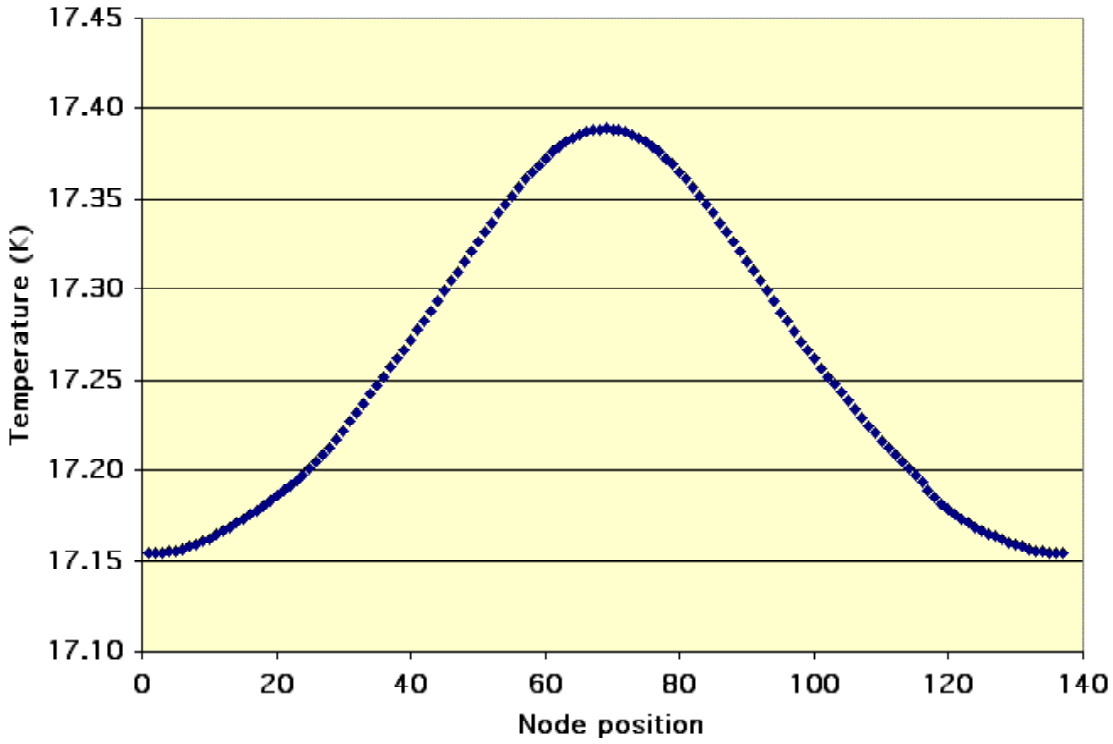

Figure 15. Imposed external temperature profile determined from the inverse solution.

Using the temperature solution along the hohlraum surface obtained in this way, the original thermal model was solved once again. Figure 16 shows the resulting temperature profile along the DT outer surface. The variation was reduced from 10 mK to less than 200 μK. Figure 17 shows the corresponding fuel thickness variation, which was reduced from 200 μm to less than 5 μm. Further refinements to the imposed temperature profile reduced the variation to <100 μK.

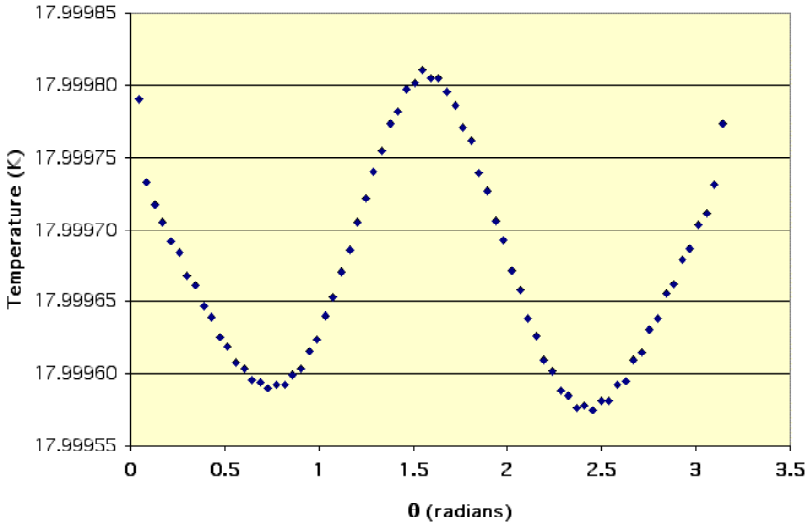

Figure 16. DT temperature profile rersulting from the applied temperatures of Figure 15.

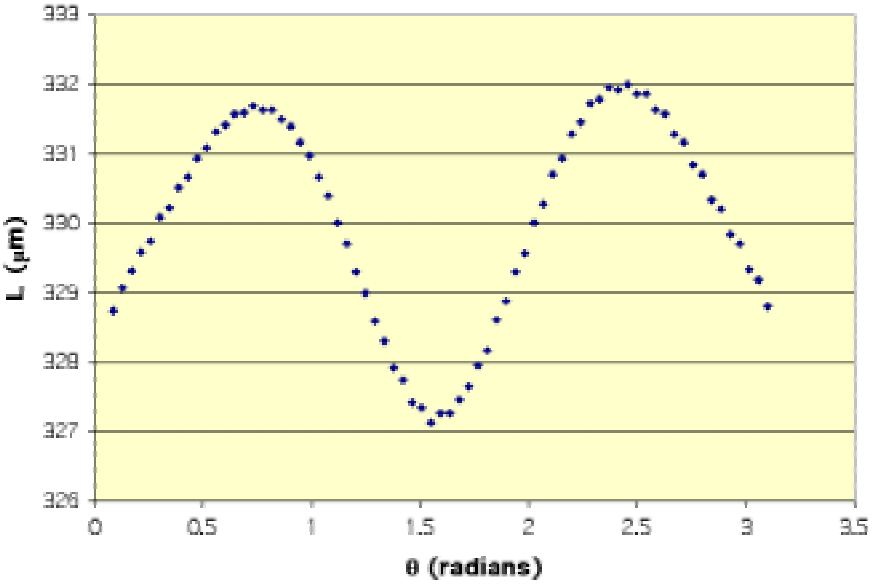

Figure 17: Variation of the DT thickness for the plastic ablator target with the applied hohlraum temperature shown in Figure 16.

2.5. Effect of Anisotropic Foams

Tailoring the material properties inside the hohlraum to achieve a uniform temperature profile at the DT surface is an alternative approach to external temperature control. Most of the materials inside the hohlraum are very low density and saturation of these foams with helium was used to assist the thermal conductivity of these regions. However, some regions (such as F, G, I, and J) have sufficient density to possibly provide higher thermal conductivity than helium in one direction. If they are made similar to layered foil insulation found in Barron [5] rather than isotropic foam, it is assumed that a desirable orthotropic effect can be achieved. By manipulating the properties of these orthotropic materials inside the hohlraum, it is thought that the heat flow can be "steered" along a more desirable path than for the isotropic case.

2.5.1. Model description

Thermal conductivity perpendicular to the foils is modeled with helium properties whereas thermal conductivity parallel to the foils is modeled based on the material density. Table 2 summarizes the properties used in the parallel direction for regions that were used in subsequent ANSYS® models; these properties were assumed constant with temperature. Calculations for determining the parallel thermal conductivity for layered foils are shown in Appendix A.

Table 2: Parallel thermal conductivity of layered foil insulations

Region	Parallel thermal conductivity (W/m-K)
A	11
E	12
F	303
G	29
I	239
J	60

Figures 18 and 19 show the models for Case I and Case II, respectively, where the thermal conductivities from Table 2 are applied in the direction of the parallel lines. Temperature dependent helium properties are used in the perpendicular direction. The remainder of the model is the same as the plastic ablator model of Section 2.3 with anisotropic properties in Region B. A constant hohlraum boundary temperature of 17 K was used for both cases.

2.5.2. Results

The objective of Case I was to try and reduce the temperature on the capsule adjacent to Region I by creating a heat flow path to the ends of the hohlraum through Regions I and J. The results are shown in Figures 20 and 21. Figure 20 shows that the temperature distribution is visibly changed from the result in Figure 9, but Figure 21 shows that the DT surface temperature profile is slightly worse (by 1 mK) than the constant temperature case with isotropic helium properties in Section 2.2.2.

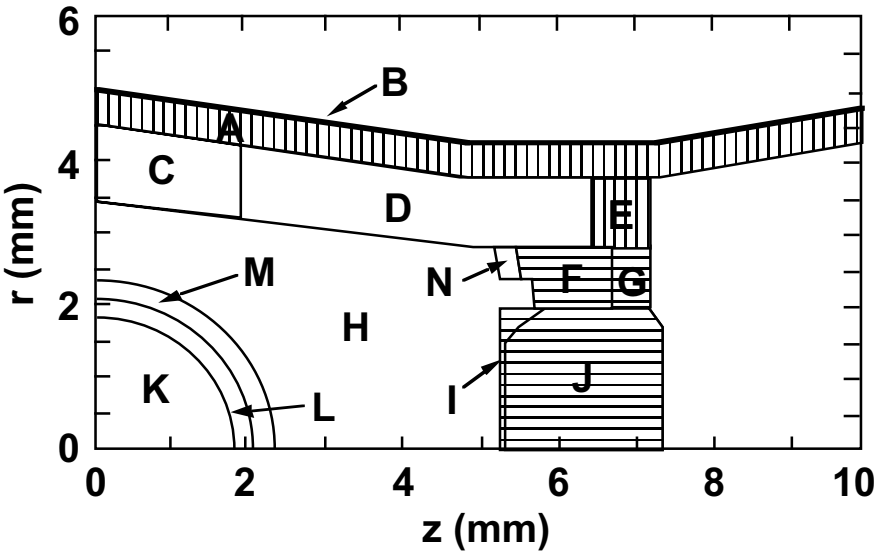

Figure 18. Model of anisotropic properties. Case I.

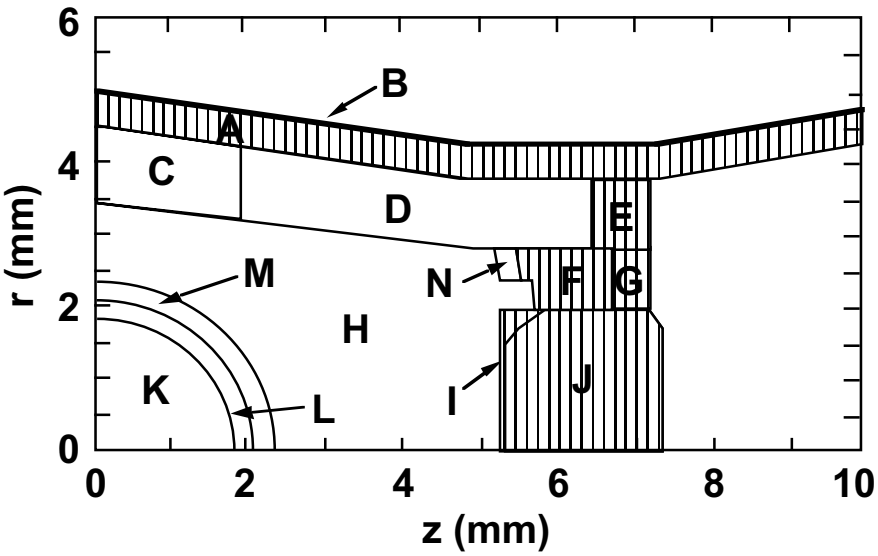

Figure 19. Model of anisotropic properties. Case II.

Regions A and E were designed to assist in removing the heat from regions F, G, and the helium blocks at the hohlraum ends since the boundaries at the ends of the hohlraum are adiabatic and all heat must flow through Region A to get to the 17 K constant temperature heat sink.

Case II was an attempt to steepen the temperature gradient adjacent to the capsule in order to accomplish the same objective of the Case I model; reduce the temperature of the capsule adjacent to Region I. Figure 22 shows a visible change in the temperature distribution, but Figure 23 shows that the DT surface temperature profile remains virtually unchanged from that of Case I.

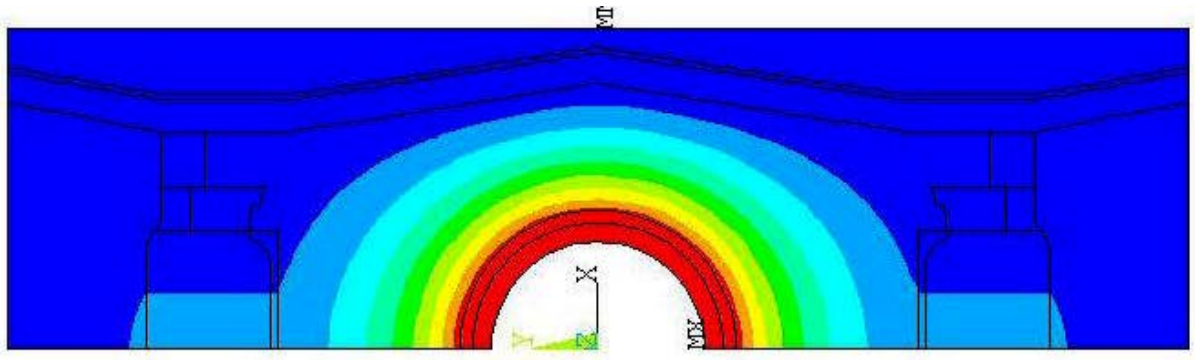

Figure 20: Hohlraum temperature distribution. Case I.

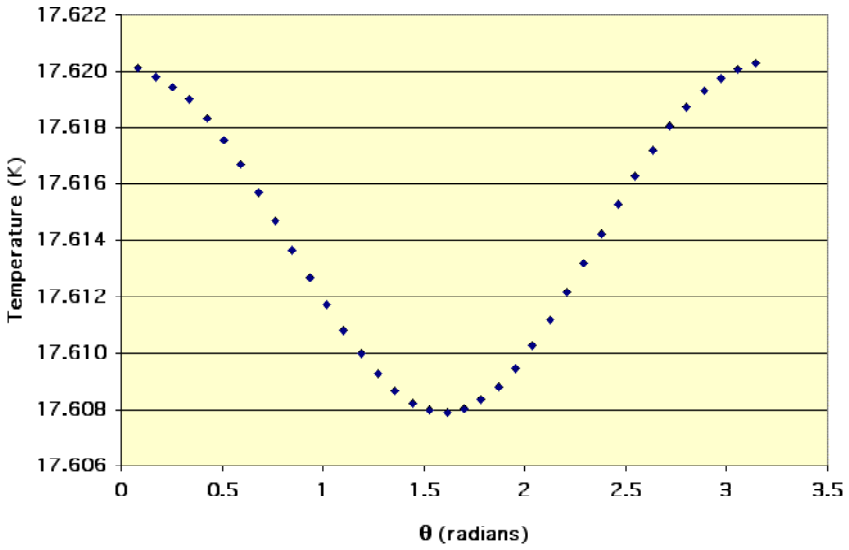

Figure 21: DT temperature profile. Case I.

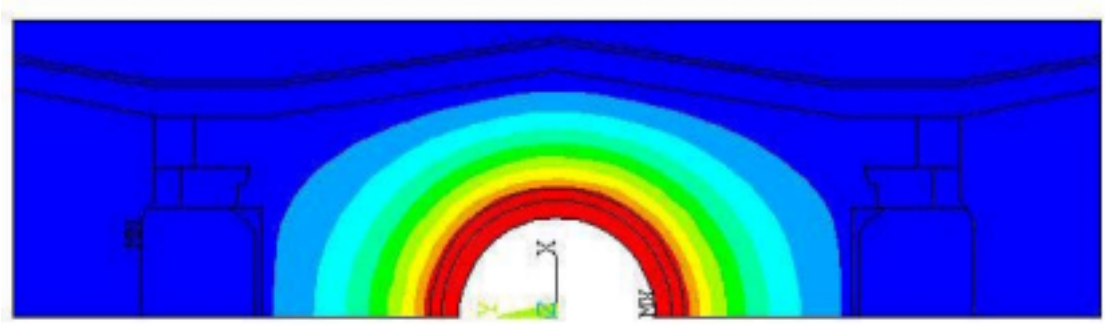

Figure 22: Hohlraum temperature distribution. Case II.

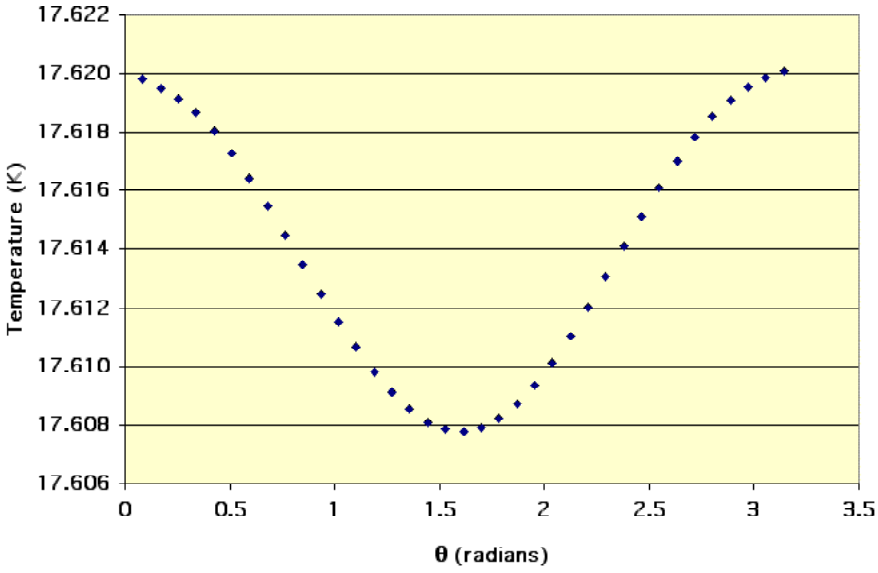

Figure 23: DT temperature profile. Case II.

2.6. Analysis of the External Control System

The reference technique for controlling the outer surface of the hohlraum is described in Section 3 of this report. It includes coolers attached to a high-conductivity outer shell (which provides a defined isothermal region), a second interior layer with thickness designed to provide the required temperature variation on the hohlraum outer surface, and a thermal contact material to minimize variations in contact conductance between the control system and the hohlraum (see Figure 24).

In order to obtain a first estimate of the insulator thickness required to map the constant copper temperature onto the desired hohlraum surface temperature, a simple estimate was made using the temperatures and heat fluxes determined in Section 2.4, and assuming one-dimensional heat flux in the insulator. Figure 25 shows the result.

Figure 26 shows the temperature distribution in the hohlraum and thermal control pipe. For this analysis, the contact resistance in the contact felt is assumed to be negligible. Figure 27 highlights the temperature variation along the DT fuel for this case. The peak variation is less than 1 mK. Further optimization of the insulator thickness profile is expected to reduce this.

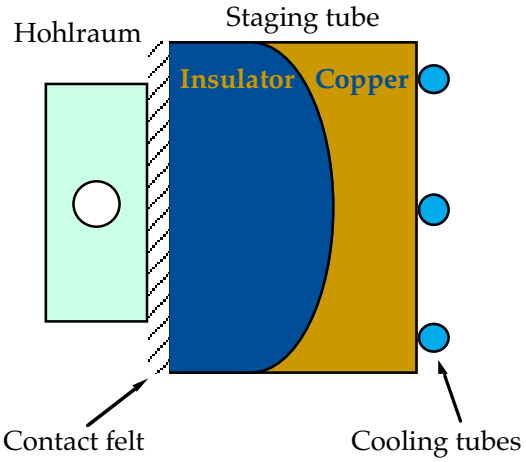

Figure 24. Passive control geometry.

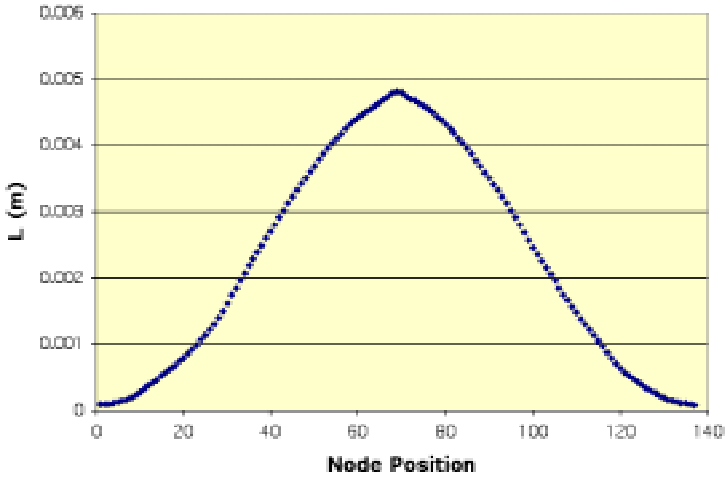

Figure 25. Estimated insulator thickness for passive thermal control.

Figure 27 is the resulting temperature at the capsule surface when the low conductivity layer of the thermal control pipe has isotropic thermal conductivity. If the interior layer of the thermal control pipe is made with anisotropic thermal conductivity (to prevent conduction in the direction along the pipe in the interior layer), the capsule temperature distribution shown in Figure 28 results. The temperature variation in Figure 28 is about half that of the case shown in Figure 27.

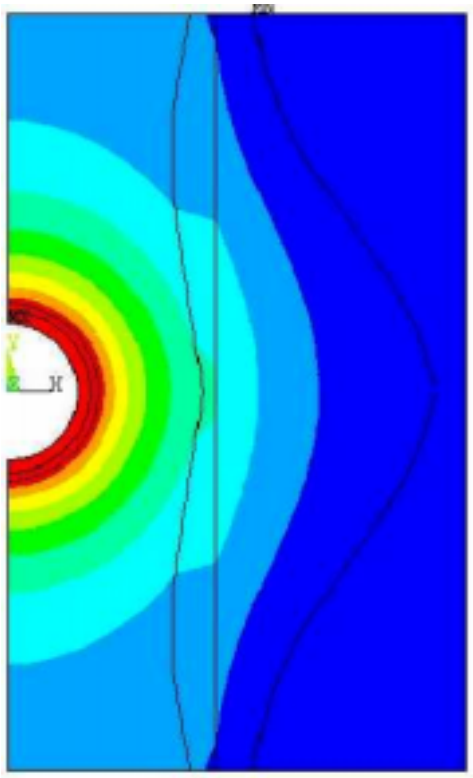

Figure 26. Temperature profile in the hohlraum and thermal control pipe.

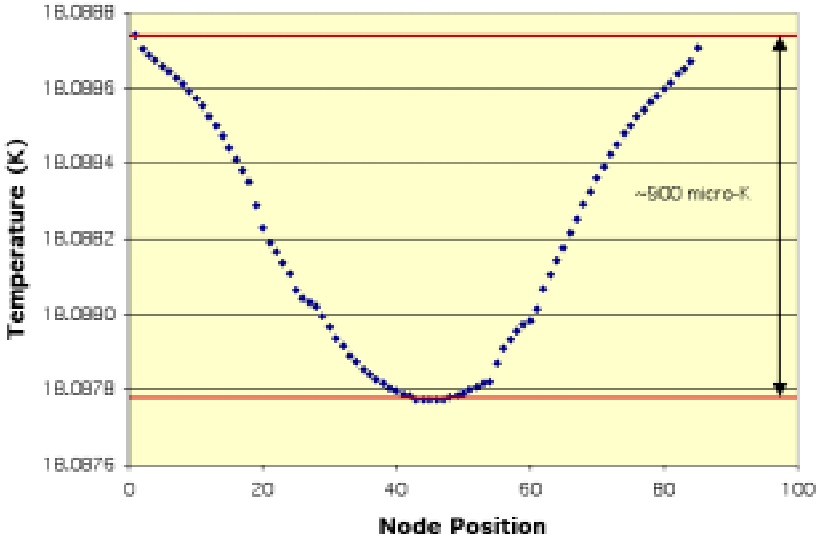

Figure 27. Temperature profile along the DT surface using the thermal control pipe.

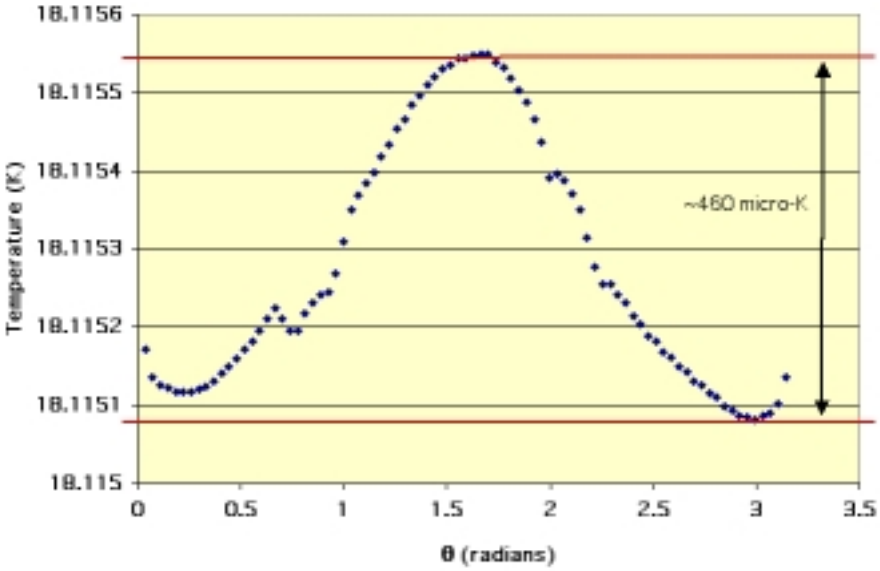

Figure 28. Results using k_x=0.0125, k_y=0 for the interior layer of the cryotube. (x is the radial direction of the cryotube and y is the axial direction).

2.7. Sensitivity Studies

Variations to the reference case were studied in order to determine the sensitivity of the result to small perturbations. Three types of perturbation were examined: 1. changes in hohlraum material properties, 2. error in the temperature profile applied to the hohlraum outer surface, and 3. uncertainty in the position of the hohlraum in the staging tube.

2.7.1. Variations in thermal conductivities

Variations in thermal conductivities of the hohlraum materials were found to have some effect on the DT temperature profile in *Section 2.5*. Using the plastic ablator model with anisotropic properties in Region B from *Section 2.3*, Region D is selected on one end of the hohlraum in order to vary its properties slightly from that of helium. Figure 30 shows the result of a +/- 1 % change in thermal conductivity of Region D labeled in green in Figure 29. Figure 31 shows the result of a +/- 10% change in the thermal conductivity of Region D.

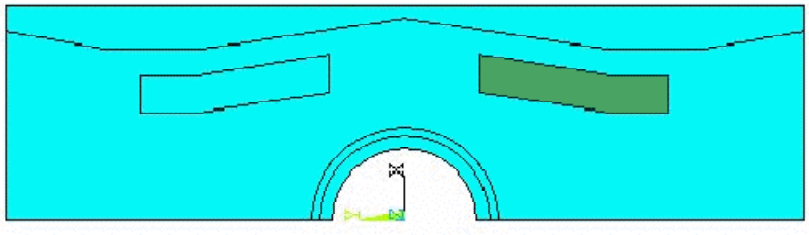

Figure 29. Zone D.

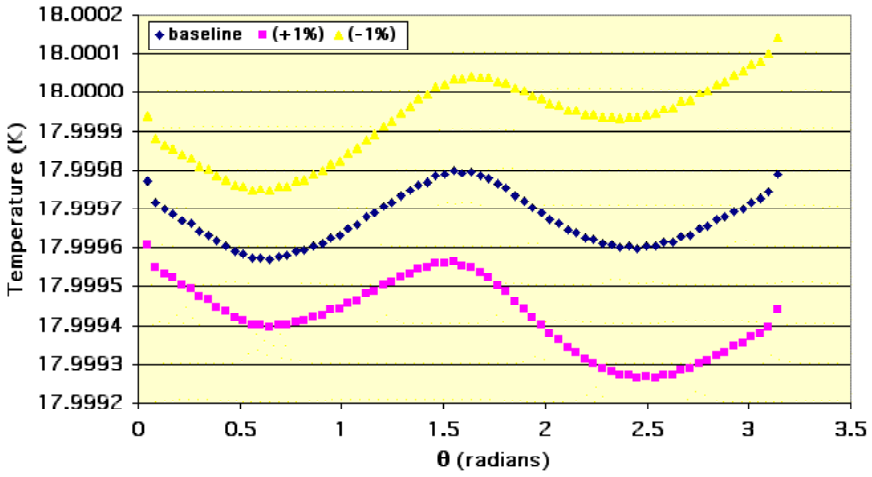

Figure 30. DT outer surface temperatures from +/- 1% change in Zone D conductivity.

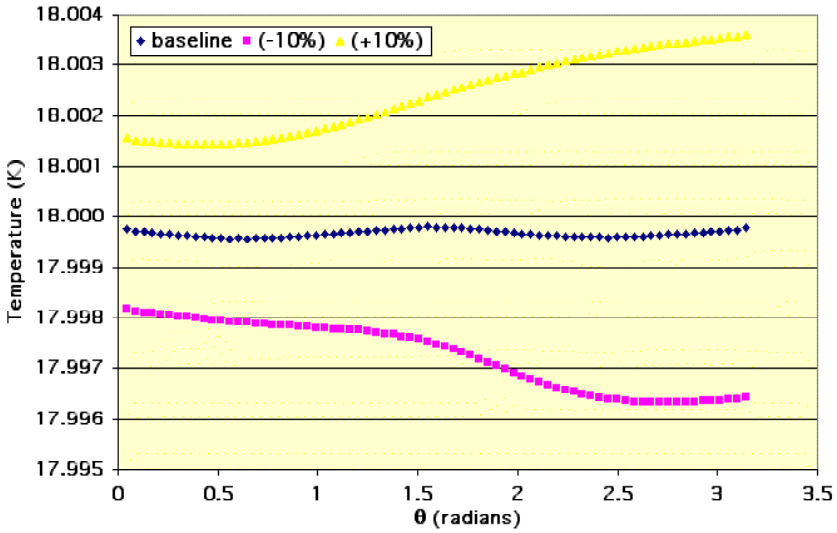

Figure 31. DT outer surface temperatures from +/- 10% change in Zone D conductivity.

2.7.2. Variations in temperature profile along the hohlraum outer surface

The effect of errors in the thermal control system is analyzed by perturbing the input temperature profile of Figure 15. A 10% error in the peak temperature as shown in Figure 32 was used as input and the results are shown in Figure 33. A 900 μK temperature difference results at the surface of the DT as opposed to 200 μK reported in Figure 16.

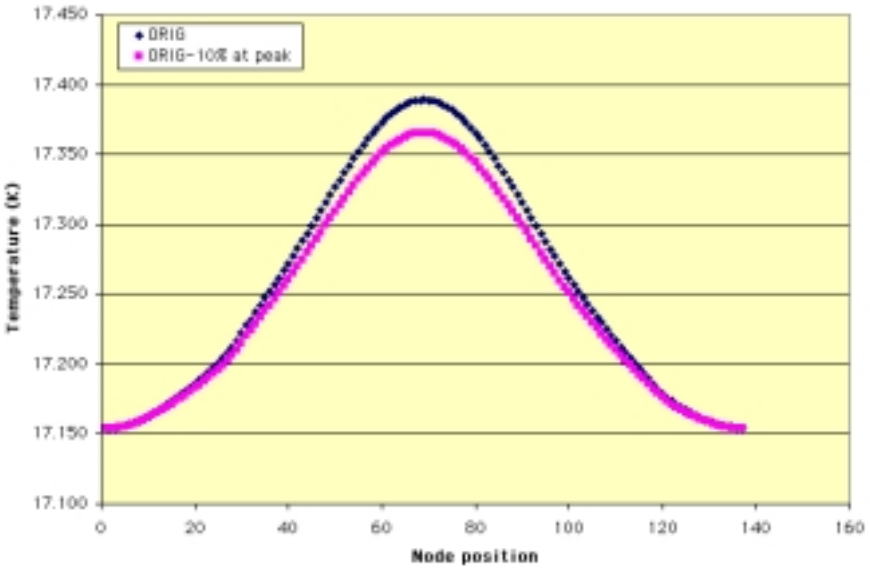

Figure 32. Temperature input profiles (blue line is same as Figure 15).

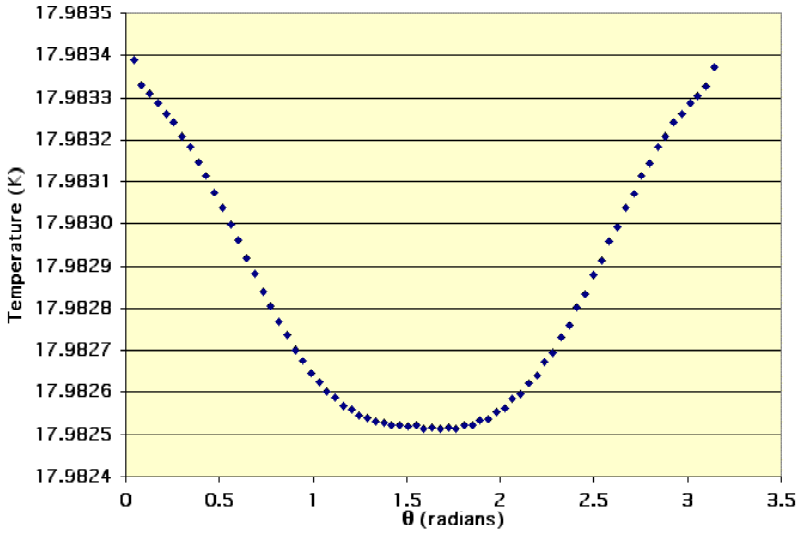

Figure 33. DT outer surface temperatures from - 10% change in peak input temperature.

Attempts were made to adjust the input temperature profile in order to reduce the capsule surface temperature variation below the 200 μK result achieved directly from the inverse problem. After some trial and error, the manually generated input temperature profile shown in Figure 34 resulted. This manually generated set of input temperatures produced the capsule temperature distribution shown in Figure 35. The manually generated input temperature profile demonstrates that 100 μK capsule surface temperature variation is possible.

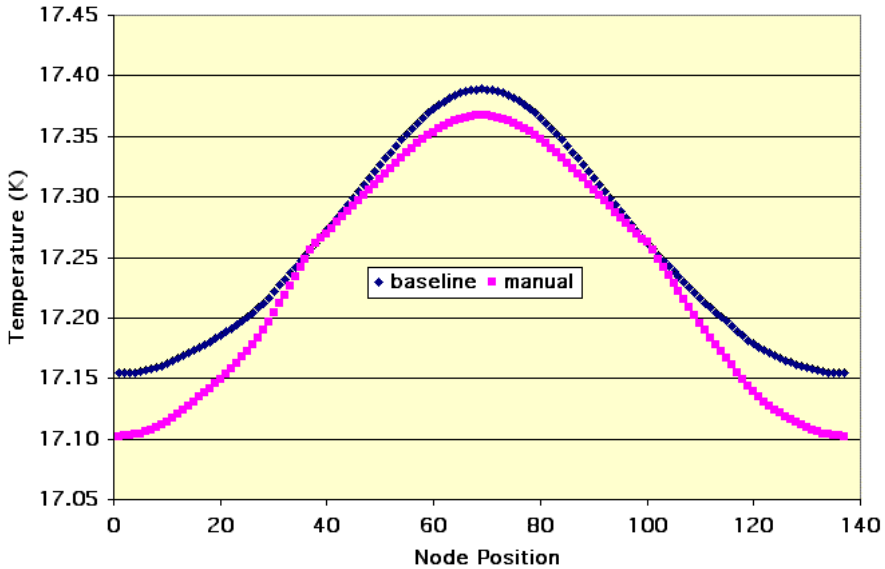

Figure 34. Comparison of baseline input temperatures from inverse problem with manually derived input temperature profile.

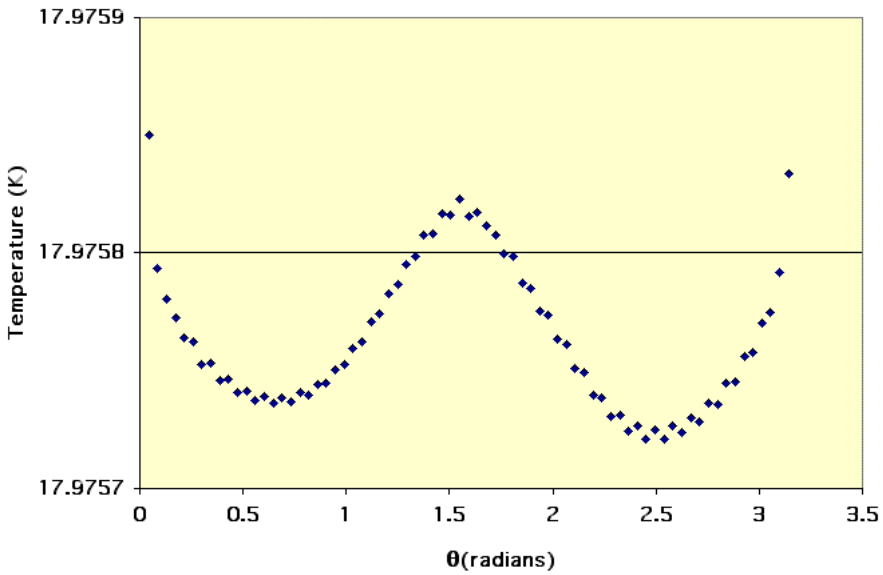

Figure 35. Result of application of manual input profile: capsule temperature distribution.

The manually generated input temperature profile used trial and error to correct the mode 2 perturbation of the capsule temperature distribution. Automation of this procedure with a computer algorithm that reads the baseline capsule temperature distribution and makes corrections to the input temperature profile based on the temperature error at the capsule was thought to be a better approach at smoothing the capsule temperatures. A computer program was written that reads the baseline capsule temperatures, normalizes, and maps them to the hohlraum surface with a spline fit. The program also reads in the baseline hohlraum temperatures and adjusts them using feedback from the capsule "error". Further refinements were made to the program in order to account for the mapping from a circle to a line by using a weighting parameter, w, that adjusts the amplitude of the feedback response according to the distance between the capsule and the hohlraum surface. The corrected hohlraum temperature distribution is used as input to the ANSYS® model which then produces new capsule temperatures. The procedure is iterated until convergence.

A resulting hohlraum input temperature profile is shown in Figure 36 and compared with the original profile resulting from the inverse problem (Fig. 15). Figure 37 shows the capsule surface temperatures that result from solving the ANSYS® model with the input profile in Figure 36. This profile (using the automated procedure) shows approximately the same amount of error as the manual procedure.

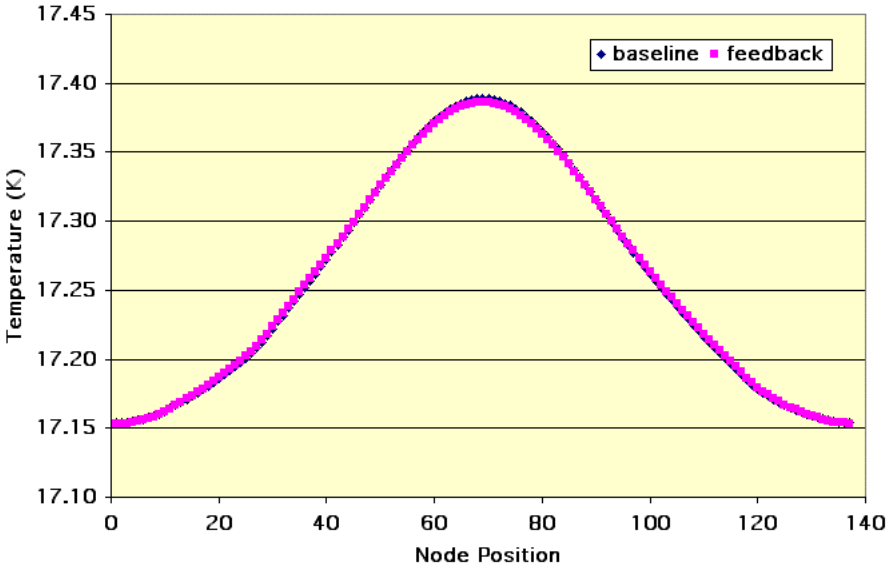

Figure 36. Comparison of inverse problem input with feedback corrected input (blue line is same as Figure 15).

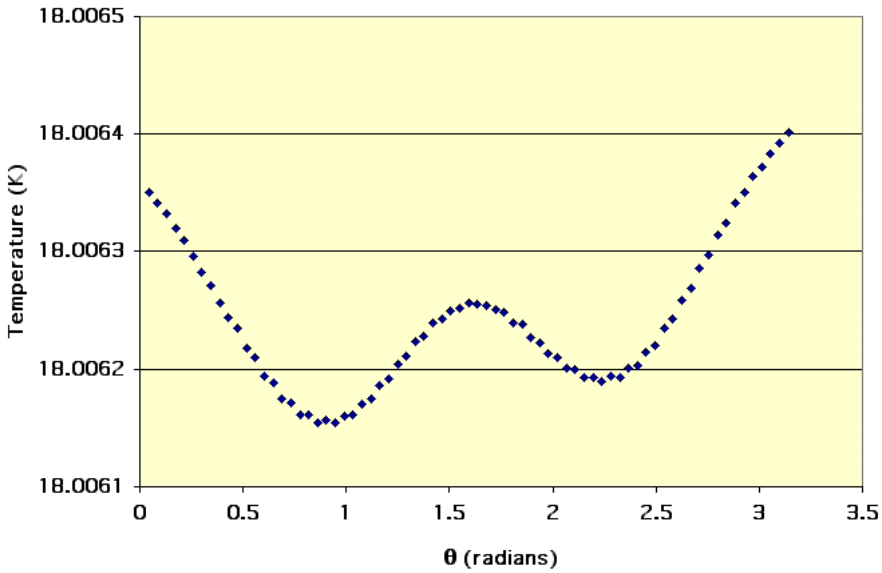

Figure 37. Resulting capsule temperatures from feedback-corrected input temperature profile.

2.7.3. Variations in target location

The passive thermal control technique requires a hohlraum to be properly aligned in the scalloped cryotube to insure correct thermal control. The effects of a 10-micron and a 20-micron shift of the hohlraum are shown in Figure 38. The baseline temperature variation along the DT is 200 μK. A 10 μm shift of the hohlraum index from the correct position in the cryotube adds another 100 μK variation for a total 300 μK temperature variation. A 20 μm shift results in about 450 μK total temperature variation along the DT inner surface.

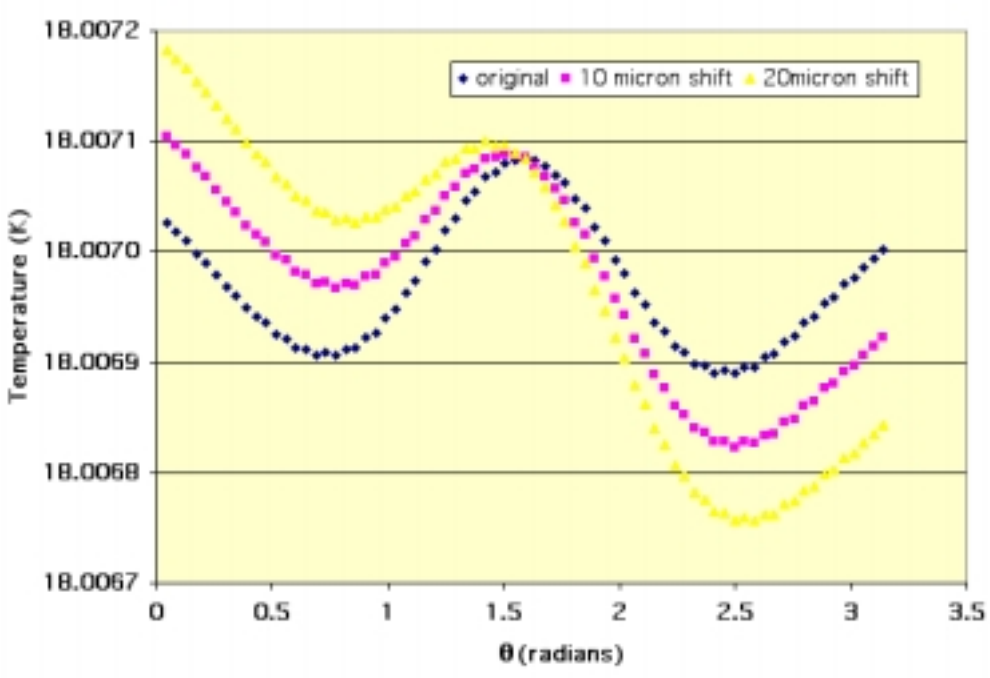

Figure 38. Change of DT inner surface temperature profile due to shifts in hohlraum position.

3. Design of the Cryogenic Control System

The purpose of the work in this section is to evaluate the applicability of the in-hohlraum approach to mass-production use. A single DT capsule during the layering process generates 0.754 mW due to tritium decay which must be removed by the Target Fabrication Facility (TFF) cryogenic systems. Assuming a throughput rate of 6 Hz and assuming the layering process takes 3 hours and there is a 30 minute "buffer" supply of prepared hohlraums, the total inventory of hohlraums in-process at one time is 75, 600. The delivery system must process approximately 20,000 hohlraums per hour.

Figures 39 and 40 illustrate the delivery system that removes capsule heating during layering. The system consists of a cryogenic carousel about 1 meter in diameter containing 18 bundles of hohlraums. Each bundle in turn contains 18 stacks of hohlraums. Each stack is 4.68 m long and holds 234 hohlraums. Two 0.25" cooling tubes are brazed vertically on each stack. Helium is supplied at 16 K and 100-200 psia. The helium flow characteristics per stack are: 0.3 g/s, 0.1 K temperature rise bottom/top and 10 psi pressure drop.

By simultaneously indexing the bundles and carousel, a stream of hohlraums at 6 Hz can be fed to the final delivery tube while maintaining a time-between-movements of 54 seconds during most of the layering process.

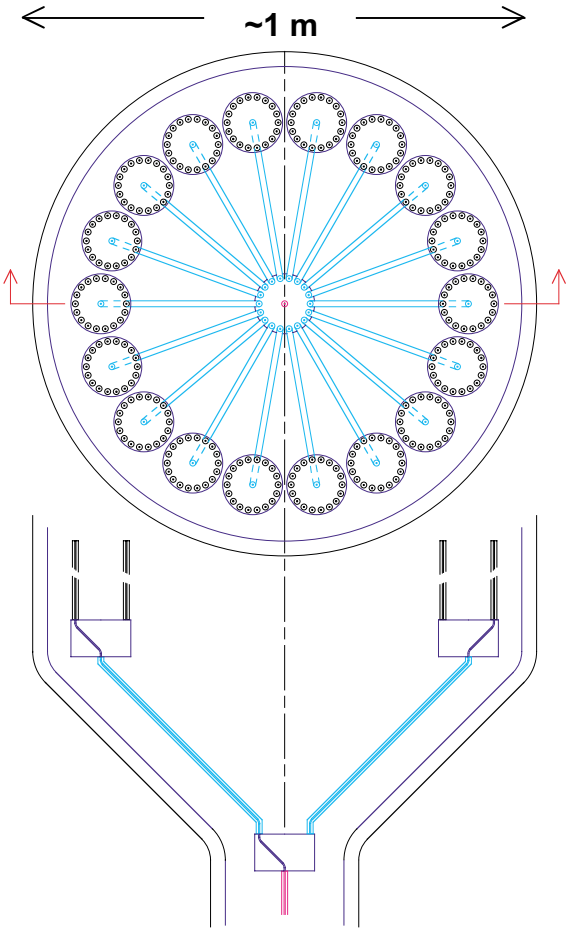

Figure 39. Schematic of cryogenic carousel for delivery of approximately 20,000 layered hohlraums.

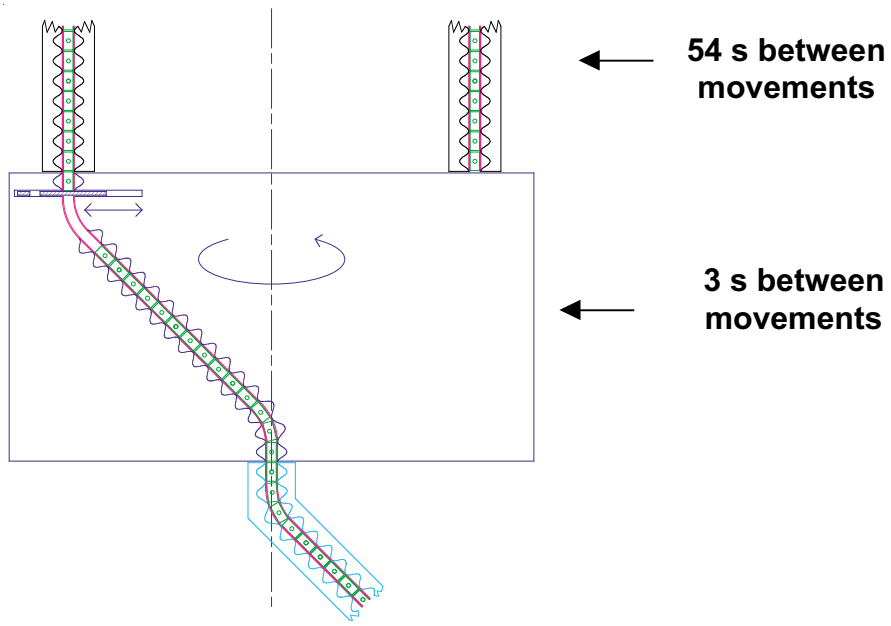

Figure 40. Cutaway of cryogenic carousel illustrating use of rotating portion to cause increasing rate of movements between hohlraum positions.

4. Conclusions and Recommendations

In this report we have demonstrated through extensive analysis that in-hohlraum layering is possible *in principle*, but that variations in dimensions, alignments and material properties can easily cause the capsule temperature nonuniformity to exceed values needed to assure proper fuel layering. We believe that the concept shows sufficient promise to warrant continued investigation.

Analysis alone cannot demonstrate the feasibility of in-hohlraum layering. One of the most basic and important experiments is the measurement of the properties of hohlraum materials. Such measurements must be performed with sufficient accuracy to demonstrate predictability and repeatability to the level of precision needed to maintain thermal control.

Fabrication of hohlraums, the structures which contain them during the staging process and the alignment system also must be demonstrated. Again, predictability and repeatability are the most important characteristics which must be demonstrated. In addition, the ability to tailor properties, for example by imposing significant anisotropic conductivities, should be investigated.

Increased interactions between target designers and target system developers will help assure that target designs enable effective and reliable thermal control. We recommend design activities that involve both target designers and target system developers in order to explore design variations which improve the prospects for in-hohlraum layering and meet the stringent requirements of target implosion physics. If possible, tradeoffs between target gain and target design modifications should be considered; by considering tradeoffs rather than rigid requirements, a feasible design space is more likely to emerge.

In-hohlraum layering appears to be incompatible with accelerated layering via rf heating techniques, as has been proposed for direct drive targets. Alternative methods for accelerated layering should be explored. This may require additional modifications to the target design in order to enable energy transfer into the DT fuel.

ACKNOWLEDGEMENTS

This work was supported by the U.S. DOE under Grant No. DE-FG03-00ER54595.

REFERENCES

1. D. A. Callahan-Miller and M. Tabak, "A Distributed Radiator, Heavy Ion Driven Target Driven by Gaussian Beams in a Multibeam Illumination Geometry," *Nuclear Fusion* **39** (7), July 1999.

2. Hoffer, J.K. and L.R. Foreman, "Radioactively Induced Sublimation in Solid Tritium," *Physical Review Letters* **60** (13) March 28, 1988.

3. M. C. Herrmann, M. Tabak, D. A. Callahan-Miller and J. Lindl, "Surface Finish Requirements for IFE," presentation at the Indirect Drive Target Workshop, General Atomics, San Diego, May 1, 2001.

4. N.P. Siegel, “Thermal Analysis of Inertial Fusion Energy Targets,” San Diego State University Thesis, May 30, 2000.

5. Randall F. Barron, Cryogenic Systems. New York: Oxford University Press, 1985.

Appendix A. Properties

Helium thermal conductivity (Table 1) is used for the perpendicular thermal conductivity of the multi-layer insulation in Section 2.5. However, much lower values for the perpendicular thermal conductivity can be attained in a vacuum (a typical value is 0.00008 W/m-K).

Table 1. Thermal Conductivity of Helium gas [1]

Temperature, K	k, W/m-K
14	0.02067
16	0.02435
18	0.02435
20	0.02582
25	0.02962
30	0.03330

Thermal conductivity in the direction parallel to the layers of multi-layer metal foil insulation is typically 3 orders of magnitude higher than in the direction perpendicular to the layers [2]. Parallel thermal conductivity depends on the overall density of conducting material present in a given region and is calculated simply by multiplying the percent density of the conducting material in the region by the thermal conductivity of the fully dense material [3]. Results are shown in Table 2 and are reported for a temperature of 20 K.

Table 2. Thermal Conductivity parallel to layers in anisotropic regions at 20 K

Region	Density (mg/cm^3)	Full Density (mg/cm^3)	% density	Fully dense k (W/m-K) [3]	Parallel k (W/m-K)
A	100	13,500	0.74	1,500(Au)	11
C	16	7870	0.2	997 (Fe)	2
D	11	13,500	0.08	1,500(Au)	1
E	110	13,500	0.82	1,500(Au)	12
F	70	2702	2.59	11,700(Al)	303
G	260	13,500	1.93	1,500(Au)	29
I	55	2702	2.04	11,700 (Al)	239
J	533	13,500	4	1,500 (Au)	60

References:

1. Y.S. Touloukian, S.C. Saxena, P.E. Liley, Thermal Conductivity-Nonmetallic Liquids and Gases. Vol. 3 of Thermophysical Properties of Matter. New York: IFI/Plenum, 1970.

2. Barron, Randall F., Cryogenic Systems. New York: Oxford University Press, 1985.

3. Y.S. Touloukian, R.W Powell, C.Y. Ho, P.G. Klemens, Thermal Conductivity – Metallic Elements and Alloys. Vol. 1 of Thermophysical Properties of Matter. New York: IFI/Plenum, 1970.